Application of thermal imaging for estimating current yield in the apple orchard

D. Stajnko, M. Lakota, M. Hočevar and Z. Čmelik

Anwendung der Thermalbildanalyse für die Bestimmung des momentanen Ertrags in einer Apfelanlage während der Vegetation

1. Introduction

Forecasting the number of fruits and size at harvesting represents the basis for prediction of future yield, forming of prices and planning storing capacities for apples (WINTER, 1986). On the basis of a long term orchard experiment at the Bavendorf Research Station, Professor Winter introduced the 'Frupro' Crop Forecast Model in practice (WELTE, 1990). The model is based on the yield capacity of the observed growing unit (tree, variety, rootstock, orchard age and exposition, area), the fruit-set density of the growing unit in the given year and the average fruit mass at harvesting (WINTER, 1979). Nowadays, his improved method known as 'Prognosfruit model' has been used for estimating yield in many European countries.

Currently, the Prognosfruit Forecast Model is the only method for yield quantity and quality estimation accepted by the European apple and pear producers. The method successfully predicts future yield for large growing areas or countries with similar environmental condition, while for more variable conditions differences between the forecast and harvested yield from -21,9 % to +14,1 % per hectare has been reported (LAMBRECHTS, 2001).

However, the main disadvantage of the method characterised are time-consuming measurements of required parameters, which are needed for determining the future yield. Possible improvement in data measurements for such forecasting methods can be achieved by applying visual and heat sensing techniques in collecting of samples.

The machine vision represents one of the image processing tools that have been used for various agricultural applications by providing information about plant size,

Zusammenfassung

Ziel der hier vorgestellten Arbeiten ist es, neue methodische Ansätze zu beschreiben, bei denen die thermalbildanalytische Klassifikation von Apfelzahl, Apfeldurchmesser und Apfelertrag vollautomatisch unter Praxisbedingungen bestimmt werden. Die Thermalkamera wurde am Rahmen des Traktors befestigt und mit einem PC verbunden. Im Laufe der Vegetation von Juni bis September wurden die Bilder von zwanzig Apfelbäumen vier Mal aufgenommen. Jedes Mal wurden zwei Serien von Bildern gemacht, d.h. eine Serie von der Sonnseite der Baumreihe und die andere von der Schattseite. Der Bilddatentransfer erfolgte schon auf dem Traktor über eine digitale Framegrabberkarte. Alle Bilder wurden dann (off-line) mittels unterschiedlicher Bildalgorithmen verarbeitet. Es konnte gezeigt werden, dass mit diesem thermalbildlich gestützten Ansatz bei Apfelzählungen eine gute Beziehung (R^2 von 0,76 bis 0,81) zwischen manuellen Probenahmen und Thermalbildanalysen existierte. Für die Apfeldurchmesserbestimmung wurde zwar ein geringfügig schlechtere Beziehung R^2 (von 0,56 bis 0,78) geschätzt, die aber mit der Farbe- und Durchmesserentwicklung offensichtlich stieg. Wenn man den momentanen Ertrag mittels der Thermalbilderalgorithmen beobachtet, besteht ebenfalls eine hohe Korrelation (R^2 von 0,69 bis 0,79). Eine noch bessere Beziehung (R^2 von 0,79 bis 0,89) wurde erreicht, wenn die Thermalbildanalyse mit dem gewogenen Ertrag verglichen wurde. Die Ergebnisse von den Juni- und Juliprobenahmen scheinen aussichtsreich für die weitere Entwicklung und Einführung der Thermalbildanalyse in die herkömmlichen Ertragsprognosemethoden, um ein schnelleres und präziseres Datenprobenahmesystem zu erreichen.

Schlagworte: Thermalkamera, Bildanalysis, Apfel, Fruchtzahlen, Ertrag.

Summary

The paper describes a thermal imaging based technique for estimating number, diameter and yield of apple fruits automatically under natural condition in the orchard. A thermal camera was mounted on a tool-frame tractor equipped with a PC for acquiring apple trees images four times during the vegetation period June-September 2002. Each time twenty apple trees were recorded from both sides of the row. Video signals from the camera were digitised using frame grabber and the images were processed off-line using several image processing algorithms. Correlation coefficients (R^2 from 0,78 to 0,81) were established between manually measured fruit number and estimated number based on the thermal imaging algorithm. For measuring the fruit's diameter R^2 between 0,56 and 0,65 were established and were slightly increasing according to the size development during the ripening. The R^2 for current yield per tree were estimated from 0,69 to 0,79 when manual measurements were compared to thermal imaging.

Keywords: thermal camera, image analysis, apple fruits, number, yield.

population density, plant health or fruit detection (HEMMING and RATH, 2002). Nowadays, the efficient fruit detection algorithms processed automatically all kind of fruit's characteristics in artificially lighted chambers. However, by working in the outdoor condition researchers are constantly developing new fruit recognition algorithms. By the detection of ripen apple fruits, different accuracies between 48–70 % were reported in investigations from PARRISH and GOKSEL (1977), GRAND D'ESNON et al. (1987), RABATEL (1988) and KASSAY (1992).

Contrary to the machine vision techniques, thermal cameras sense an object's own heat radiation and visualise it on the video signal or on thermal images. The intensity of thermal radiation is related to the temperature of the body with the power of four and is directly proportional to the emissivity of the sample. This allows evaluation of different characteristics of observed objects as being the way by standard visual cameras. The application of thermography for the study of plants or plant materials was reported in the determination of physiological depression (INOUE, 1990), the leaf transpiration rates (INOUE et al., 1990), differences in the flag leaf temperatures of the cereals caused by diseases (NILLSON, 1995; DALEY, 1995) as well as for the bruise detection of apple fruits (BEVERLY et al., 1987, TOLLNER et al., 1993; LINKE et al., 2000; JATUPHONG et al., 2001).

However, very few researches have been reported concerning application of thermal imaging for determining and counting fruits under the natural conditions. ZHANG et al. (1997; 1998b) investigated the potential of the infrared thermal image for distinguishing apples from trees in the orchard. The obtained results confirmed that the thermal difference between apples and leaves was over 1 °C, however the difference between apples and branches was very slight when the weather was clear and calm. During the 24 hours lasting observation it was proved that the remarkable temperature difference between apples and leaves did not exist from midnight to early morning.

By using the information on the thermal distribution differences, in their further research ZHANG et al. (1998a) developed the apple detection method based on pattern recognition by the generic algorithm. Almost all apples were reported to be successfully detected from the infrared images regardless of the differences in the light intensities and the temperature of the surroundings whether they were captured during the night or day.

In our investigation the number of fruits was determined also prior the harvesting, when colours of fruits did not differ substantially from colour of leaves. To overcome this problem, a thermal imaging followed by image analysis techniques was used instead of colour imaging.

The main object of this paper is to demonstrate and evaluate the applicability of the method for predicting the number and the diameter of the apple fruits, which is used for calculating the current yield in the apple orchard. An algorithm is presented able to threshold, count and report fruits' morphological characteristics from thermal images being recorded and digitised under natural condition in the orchard.

In the following parts of the article some basic properties of the experimental methods will be explained. Then the performance of the method is estimated by comparing the predicted and actual number of fruits and diameters.

2. Materials and Methods

During the vegetation period June-September 2002, twenty apple trees (*Malus domestica* Borkh.) were examined in

the Faculty's four year-old apple orchard (lat. 46°32' N, long. 15°33'5 E). Apple trees were planted at a spacing 3,5 x 0,7 m with the variety 'Gala' grafted on the M9 rootstock. The row was orientated from East-North to West-South. Four crucial developing stages of apple fruits were selected for recording trees during the fruit's growth and ripening:

1. stage – after June fruit drop — June 16th 2002
2. stage – three weeks later — July 7th 2002
3. stage – beginning of ripening — August 8th 2002
4. stage – harvesting — September 2nd 2002

Experiments were performed five times on each stage; at 9.00, 12.00, 15.00 and 18.00 to investigate temperature gradient needed for distinguishing fruits from leaves and the background. Two series of video signals were recorded without any additional heating. The first signal included the southern side of trees and the second one the northern side of trees, both from the distance of 3,0 m at the angle of 90° degrees to the planting row. Concurrently, on each recorded tree a round sticker was put for calculating pixel/mm ratio. All fruits were manually counted on each tree and the diameters of ten randomly sampled fruits per tree were measured by applying the sliding calliper.

Thermal camera AGEMA 570 was used for recording images. Emissivity of the object was set to 0,98, relative humidity varied from 70 % to 95 %. Resolution of the camera was 320 x 240 pixels and the temperature resolution was better than 0,5 °C. On each image approximately 1270 mm by 1020 mm of the tree area were captured. Video signals from the camera were recorded on VHS-C video tape. All images were digitised (off-line) using a National Instruments® IMAQ PCI –1408 image acquisition board with a frame grabber at a 320 x 240 resolution in a 8-bit monochrome format. The digitisation and analysis of the images were carried out with a personal computer (PC) with 350 MHz processor and 256 MB random access memory (RAM). The analogue signal from thermal camera as well the grey image after digitisation is clearly seen in Figure 1.

2.1 Fruit detection algorithm

Since the digitised images were already in a grey level format, in the first step of algorithm a global threshold was used for determining between background (soil, grass, sky) and parts of plant (leaves, fruits, branches). Sometimes leaves and fruits were separated from the background together as one object, so in the following steps the fruit separation from leaves is shown. Namely, the low temperature gradient between fruits and leaves growing inside the crown reflected in insufficient illumination gradient. Therefore, the image was grown through a morphological processing operator erosion which reduced the brightness of pixels that were surrounded by neighbours with a lower intensity, so most of the misidentified pixels not connected to the fruit pixels would not appear in the final image. This operation was repeated until the segmentation between leaves and fruits was achieved but the original shape had to remain unchanged.

In the second step the image was filtered using a specified size of kernel 3 x 3 pixels and the connectivity-8 function to remove the remaining noise. Using specified filtering, it was

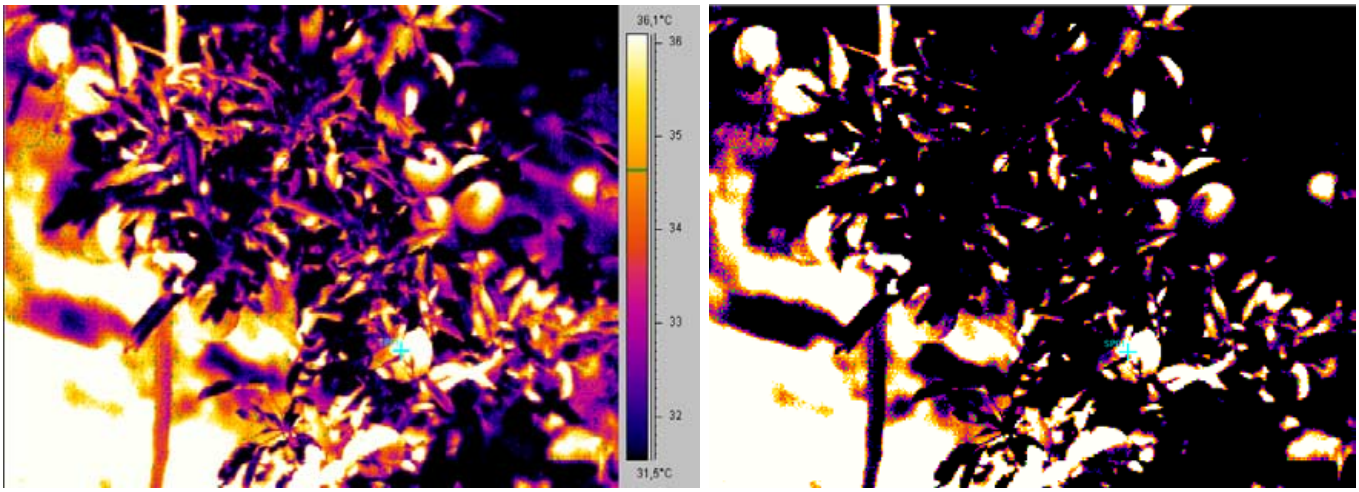

Figure 1: A sample of thermal image before (left) and after digitisation (right)
Abbildung 1: Muster eines Thermalbildes vor (links) und nach der Digitalisierung (rechts)

determined whether an adjacent pixel belongs to the same or to a different object.

For each single object obtained after the segmentation, the differentiation between leaves and fruits was proceeded according to the empirical preliminary investigations of geometrical features. The process included feature extraction, particle selection and classifier evaluation. Feature extraction adjusted horizontal and vertical resolution, while classifier evaluation calculated different shape features as: major axis, length, width, longest segment, contour length and compactness, and compared them with stored parameters. For all segmented objects in the image the membership of the class of fruit or leaf was calculated. At the end only objects fitted to the sample with the confidence of 90 % or more were classified as fruits. Sample results of detecting process and labelled fruits are shown in Figure 2.

As the whole apple fruit is rarely detected on images because it is somehow covered with other fruits as well with leaves and branches, the longest segment was considered to be the same as the fruit's true diameter.

The number of fruits on each image and the average longest segment of detected fruits per image were the basis for estimating the current yield. A file with recorded fruit characteristics as well the yield per image was stored for calculating a statistical analysis. For calculating current yield on the image the following equation was applied:

$$Y_t = \frac{N \cdot 0{,}459\ D^{2{,}9602}}{10^6} \qquad (1)$$

where Y_t represents yield per tree, N the number of fruits per tree and D average fruit diameter per tree.

Our estimation based on a transformation function derived by WELTE (1990), which allows a direct calculation of the weight from the fruit's diameter. He showed that during the fruit growing the relative increase in the diameter was proportional to the relative fruit weight increase.

For the first three samplings the average fruit yield per tree was estimated on the basis of the average fruit's diameter measured manually by the sliding calliper and compared to the estimated yield based on thermographically detected diameter. Contrary, on September 2nd all the yield was harvested and weighted as well as estimated by thermal imaging. Additionally, the correlation coefficient between estimated (current) yield and harvested yield was calculated for all stages.

For performing the above described image analysis algorithms the IMAQ Vision 5.0 and the Labview 6.i from the National Instruments® were used in our research.

2.2 Statistical analysis

The each stage's data of termographically analysed and manually measured parameters were the basis for creating linear regression models. The Pearson correlation coefficient was used to estimate the regression line and select the most favourable image series for predicting the current yield. Additionally, by analysing the slope and the offset of the regression line the linear regression equation was estimated for every stage separately. Only independent variables at the 5 % level were found to be significant.

The SPSS 10.0 Package Program was used for all statistical calculations.

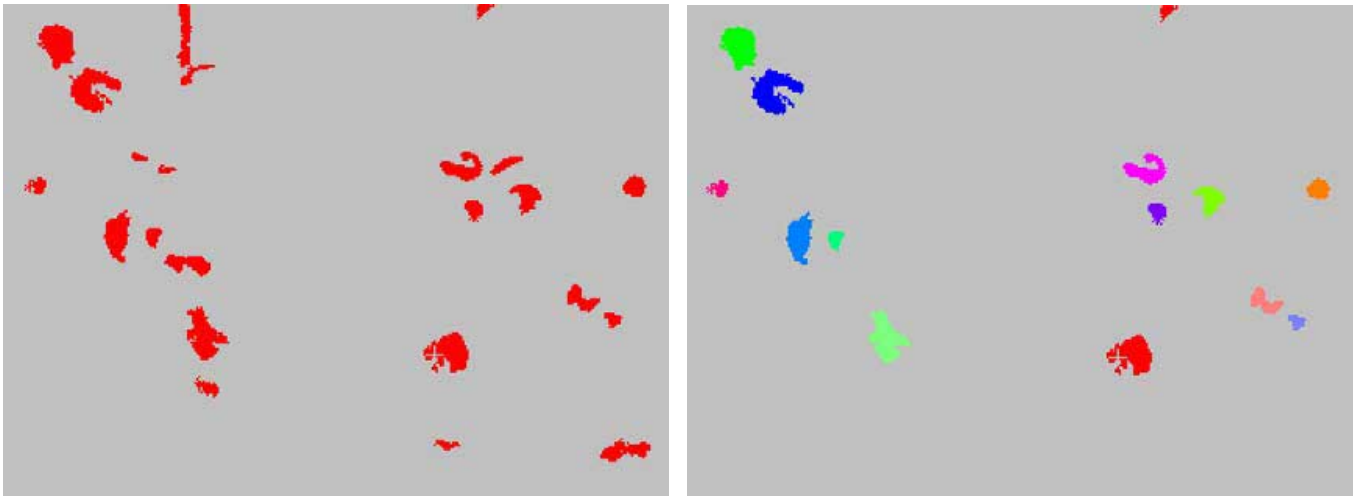

Figure 2: Binary image obtained from the Figure 1 before filtering (left) and labelled fruits after processing (right)
Abbildung 2: Aus Abb. 1 ermitteltes Binärbild vor der Filterung (links) und identifizierte Früchte nach der Verarbeitung (rechts)

3. Results and Discussion

3.1 The fruit temperature development during the day

As seen from Figure 3, showing the temperature development on the same tree during July 7th 2002, the sunlight influenced the fruit, leave and branch temperature, so it varied between 24 and 40 °C throughout the entire crown. On thermal images captured from the southern as well as from the northern side of the tree row the constant increase in the temperature could be detected between 9.00 and 15.00. However, as earlier reported by ZHANG et al. (1997) the very small temperature gradient was detected between fruits and leaves on the northern side of the tree row due to the reflective heating, which contrary to the direct sunlight could not affect the higher temperature difference.

3.2 The number of fruits per tree

Because of the variation in the fruit temperature throughout the tree (Figure 4), the thermal camera had to be set onto the average spot temperature before the signal was sent to the grabber. Once all series of images were captured, additionally, a global threshold was trained with one or two images from each image data set before the fruit detection algorithm was processed. Figure 5 shows results of image processing on the captured thermal image.

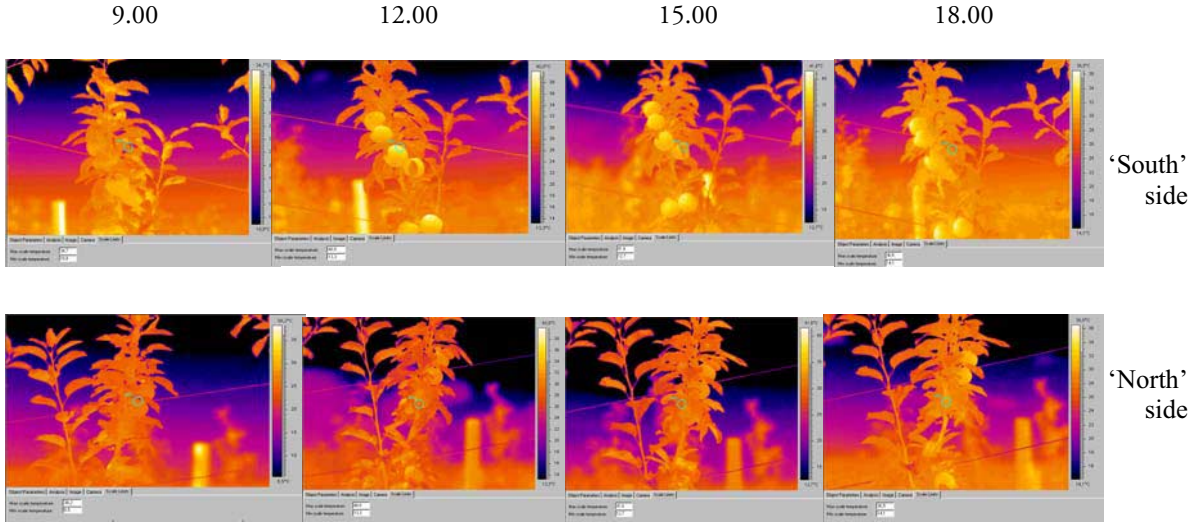

Figure 3: Thermal images captured from opposite sides of the tree at different time during July 7th 2002
Abbildung 3: Von nördlicher und südlicher Seite aufgenommene Thermalbilder des Baumes am 7. Juli 2002

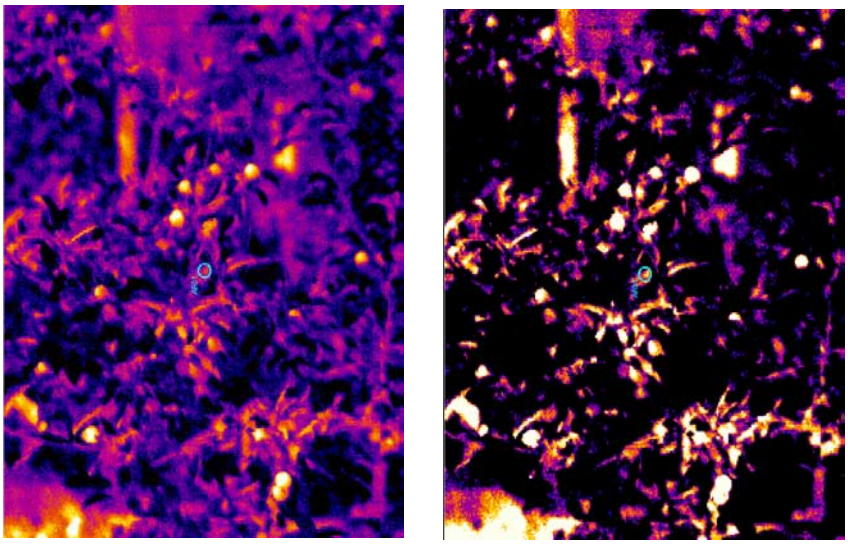

Figure 4: Original (left) and adjusted thermal image (right) showing the different temperature across the tree
Abbildung 4: Ein originales (links) sowie verarbeitetes Thermalbild (rechts) zeigen deutlich die Temperaturdifferenz über den ganzen Baum

The closer correlation coefficients were estimated on the 'southern' 12.00 image series, therefore only results of these series will be discussed in the following sessions.

The number of apple fruits per tree detected by the image analysis as well as manually counted fruits is presented in Table 1. As seen, the fruit detection algorithm was tested on differently abounded trees with 21 to 63 fruits.

The estimated correlation coefficient varied between 0,78 and 0,81. A close correlation between detected and manually counted number of fruits at the harvesting were reported also from KONDO et al. (1998) by strawberry harvester and KATAOKA et al. (1999) by apple harvesting. However, in their cases, at the beginning of ripening a weaker accuracy was caused by lack of fruit colour difference between

Table 1: Number of apple fruits per tree measured by thermal imaging and manual measurement at the different observing terms
Tabelle 1: Geschätzte Apfelanzahl pro Baum bestimmt mit Thermalbildverarbeitung sowie manueller Probenahme zu verschiedenen Terminen

Tree number	Number of apple fruits per tree							
	June 16th 2002		July 7th 2002		August 8th 2002		September 2nd 2002	
	Thermography	Manually	Thermography	Manually	Thermography	Manually	Thermography	Manually
1	28	36	34	34	31	34	34	28
2	55	65	62	63	55	53	52	55
3	27	23	27	23	22	23	23	23
4	48	60	56	57	46	48	36	48
5	53	50	49	49	48	48	45	48
6	35	38	38	38	30	34	32	32
7	48	60	42	60	50	55	60	48
8	27	27	29	24	29	24	23	22
9	36	36	44	34	29	34	34	32
10	31	38	33	37	24	36	37	31
11	37	57	48	48	43	48	42	42
12	19	21	28	20	33	20	20	19
13	29	35	39	33	35	33	33	29
14	29	27	31	25	15	23	25	23
15	66	66	36	52	44	44	52	44
16	29	31	32	30	35	30	30	29
17	9	23	22	21	17	17	12	17
18	35	31	35	31	37	31	31	30
19	55	62	60	61	53	52	71	52
20	42	52	49	50	42	42	50	42
Average	37	41	39	39	36	36	37	34
R^2	0,81		0,78		0,79		0,81	
Equation	Y = 4,65+1,00X		Y = -4,91+1,12X		Y = 4,12+0,90X		Y = 7,84+0,72X	

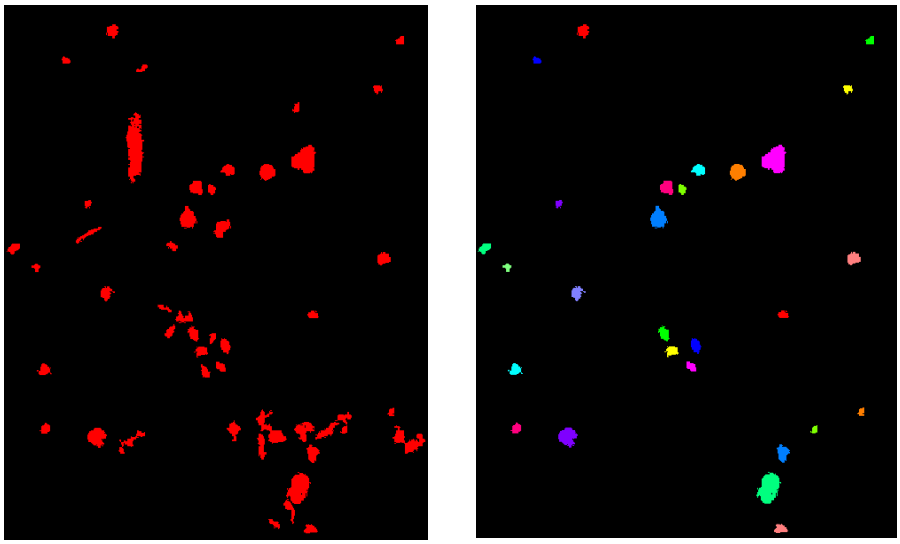

Figure 5: Thermal image after thresholding (left) and fruit detection (right)
Abbildung 5: Ein Thermalbild nach der Segmentierung (links) und Äpfelidentifikation (rechts)

leaves and fruits. In our research a closer correlation for smaller and less coloured fruits was estimated, while opposite to the cited authors using visual light, fruits can accumulate more heat than leaves, so they can be better detected by thermal imaging.

3.3 The apple fruit's diameter per tree

The average estimated fruit's diameter per tree at different developing stages of apple fruits are shown in the Table 2. As seen, the average estimated diameter per tree was equal to the manual measurements at all developing stages during the vegetation, however the correlation coefficient R^2 varied from 0,56 to 0,65.

The reason for lower correlation coefficients lies in a levelling diameter among all sampled trees, so even the small deviation in the diameter affected the great fall of the correlation. Such conditions were caused by chemical fruit thinning, which was applied in the orchard at the end of May to reduce the over abundance. However, as seen from the results, on some trees the estimated diameter was underestimated anyway. The reason lies in the fruit detection algorithm, which based on the longest segment measurement. Namely, this procedure is accurate if a whole apple fruit is detected or a part of it is clearly seen, otherwise a weaker correlation coefficient is calculated.

On the other hand, when comparing the development of fruit diameter through the entire sampling period, the high accuracy of the obtained results can be found. As seen from Figure 6, actually the same curve was obtained (R^2 = 0,90) by manual measurements as well as by thermal imaging. The estimated development of the fruit diameter was very similar to researches reported by WELTE (1990). Thus, our research shows the significant possibility of thermal imaging for predicting the fruit's diameter growing.

3.4 Estimation of fruit yield

The current yield per tree was estimated by applying equation 1. The number of fruits and the average fruit diameter from each developing stage were used for estimating yield, when the thermal imaging procedure was applied. For estimating the yield manually, measurements were used only for the first three stages, while for the last measurement all

Table 2: Average diameter of apple fruits per tree in mm measured by thermal imaging and manual measurement at the different observing terms
Tabelle 2: Geschätzte Mittelapfeldiameter pro Baum bestimmt mit Thermalbildverarbeitung sowie manueller Probenahme an verschiedenen Terminen

Tree number	Average diameter of apple fruits per tree							
	June 16th 2002		July 7th 2002		August 8th 2002		September 2nd 2002	
	Thermography	Manually	Thermography	Manually	Thermography	Manually	Thermography	Manually
1	52	51	65	63	74	75	81	79
2	57	57	60	62	72	73	80	81
3	57	54	61	60	72	72	76	77
4	53	53	62	62	72	71	78	79
5	51	55	59	61	74	74	78	79
6	52	54	63	63	74	74	78	78
7	58	58	61	61	72	72	77	76
8	57	58	65	64	76	74	76	76
9	55	54	63	61	74	74	81	79
10	52	51	65	65	75	75	81	81
11	57	55	65	64	76	75	78	79
12	50	51	67	68	74	74	77	76
13	57	57	54	61	73	73	79	78
14	58	58	66	66	77	77	77	76
15	54	54	63	63	71	71	80	81
16	57	54	63	62	77	75	78	77
17	52	53	60	59	75	75	77	77
18	52	51	63	63	70	70	77	77
19	54	54	59	61	72	73	78	79
20	52	55	63	64	68	73	78	78
Average	54	54	63	63	73	73	78	78
R^2	0,56		0,55		0,64		0,65	
Equation	Y = 7,27+0,86X		Y = 29,24+0,54X		Y = 30,65+0,58X		Y = 18,39+0,77X	

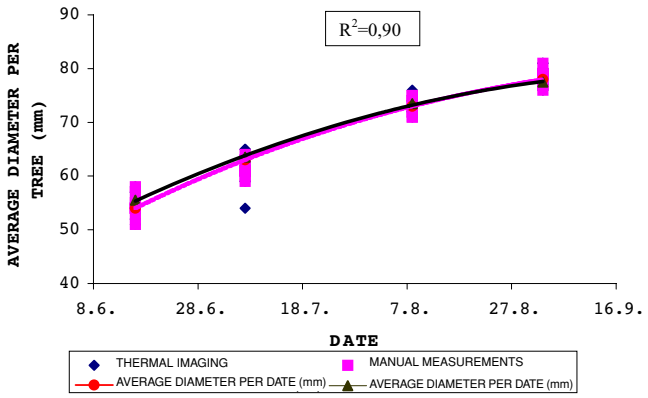

Figure 6: Growth curve for the development of the average diameter estimated by thermal imaging and manual measurements

Abbildung 6: Vergleich der Wachstumskurven der mittleren Apfeldurchmesser bestimmt mit Thermalbildverarbeitung sowie manueller Probenahme zu verschiedenen Terminen

fruits were harvested and weighted. As seen from Table 3, the average estimated yield per tree detected by thermal imaging increased from June to September.

Nevertheless, the yield per tree was slightly underestimated, as was the number of fruits on which the equation based. The correlation coefficient between manual measurements and thermal imaging estimation varied from 0,69 in July to 0,79 in September. Contrary, the correlation coefficient between thermal imaging analysis and the harvested yield remained stable round 0,79. However, as seen from Figure 7, almost identical growth curve for the development of the average yield per tree was estimated (R^2 = 0,90) when comparing thermal imaging analysis with manual measurement. Once again thermal imaging shows a good possibility for early yield development and estimation as was earlier described by the fruits diameter forecasting.

Table 3: Estimated yield per tree measured by thermal imaging and manual measurements at different developing stages and in correlation to harvesting weight

Tabelle 3: Geschätzter Baumertrag bestimmt mit Thermalbildverarbeitung sowie manueller Probenahme zu verschiedenen Terminen

Tree number	Yield per tree (kg)							
	June 16th 2002		July 7th 2002		August 8th 2002		September 2nd 2002	
	Thermography	Manually	Thermography	Manually	Thermography	Manually	Thermography	Weighted
1	1,36	1,66	3,21	2,93	4,47	4,90	6,15	5,42
2	3,52	4,16	4,62	5,17	7,32	7,06	9,08	10,12
3	1,73	1,25	2,11	1,71	2,81	2,94	3,45	3,54
4	2,48	3,10	4,60	4,68	5,64	5,89	5,83	8,70
5	2,44	2,88	3,47	3,83	6,65	6,65	7,29	8,80
6	1,71	2,07	3,27	3,27	4,15	4,71	5,18	6,63
7	3,23	4,04	3,29	4,69	6,39	7,03	9,35	8,50
8	1,73	1,82	2,74	2,16	4,02	3,32	3,45	4,27
9	2,07	1,96	3,79	2,66	4,02	4,71	6,15	6,46
10	1,51	1,75	3,11	3,49	3,46	5,19	6,70	6,44
11	2,37	3,28	4,53	4,33	6,20	6,92	6,80	8,00
12	0,83	0,97	2,89	2,16	4,57	2,77	3,12	3,88
13	1,86	2,24	2,13	2,58	4,66	4,39	5,55	5,70
14	1,95	1,82	3,06	2,47	2,34	3,59	3,90	3,53
15	3,60	3,11	3,10	4,47	5,39	5,39	9,08	8,39
16	1,86	1,69	2,75	2,46	5,05	4,33	4,86	6,10
17	0,44	1,19	1,64	1,49	2,45	2,45	1,87	3,28
18	1,71	1,43	3,01	2,67	4,35	3,64	4,83	6,29
19	3,00	3,38	4,25	4,77	7,06	6,92	11,50	9,54
20	2,05	2,99	4,21	4,51	5,60	5,59	8,10	8,66
Average	2,07	2,34	3,29	3,33	4,83	4,92	6,11	6,61
R^2 (T/M)	0,78		0,69		0,75		0,79	
R^2 (T/W)	0,79		0,89		0,81		0,79	

T – Thermography, M – Manual, W – Weighted yield

R^2 (T/M) … correlation between thermographically estimated yield and manually measured yield on each stage

R^2 (T/M) … correlation between thermographically estimated yield on each stage and harvested yield

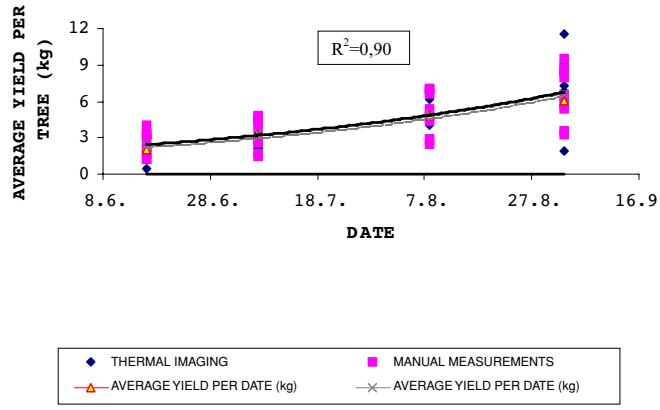

Figure 7: Growth curve for development of the average yield per tree estimated by thermal imaging and manual measurements

Abbildung 7: Vergleich der Wachstumskurven des mittleren Baumertrages bestimmt mit Thermalbildverarbeitung sowie manueller Probenahme zu verschiedenen Terminen

4. Conclusion

A new approach for counting apple fruits on trees and estimating the diameter and the current yield under orchard conditions was researched in our investigation. Video signals from a thermal camera were digitised using a frame grabber and off-line measurements were conducted by applying thermal imaging, image analysis and processing. Among image processing algorithms, thresholding, filtering and longest segment algorithm were implemented.

Estimated number of fruits, average diameter as well the estimated yield per tree, were compared to manual measurements. A close correlation (R^2 from 0,78 to 0,81) between manually counted number of fruits per tree and estimated number of fruits was determined. Therefore, the fruit detection algorithm is capable of a very good estimation of number of fruits, which was also shown by estimating the growth curve of apple fruits which actually followed manually measured data (R^2 = 0,90). A correlation coefficient R^2 from 0,56 to 0,65 was determined between manually measured and estimated fruit's diameters. Numerous apples growing inside the crown shadowed by neighbouring leaves affected relatively lower correlation coefficients, which primary reduced the accuracy of the longest segment algorithm.

For estimating average yield per tree, very close correlation coefficients (R^2 from 0,69 to 0,79) were calculated. Since the development of the fruit yield also showed a very close correlation (R^2 = 0,90), it reflected again the accuracy of algorithm for counting fruits number and measuring diameter.

Future work should be focused on improving the algorithm, so it is able to detect also partially hidden spherical objects by obtaining a set of pixels belonging to the boundaries of apples. The second goal is going to be the synchronisation between the data flow and the fruit detection procedure for processing measurements in real-time. All improvements could provide the implementation of our algorithm into advanced methods for predicting future yield, which are nowadays used in the practice, but are time-consuming and sample a relatively small part of the apple orchard.

Acknowledgements

This research was funded by The Ministry of Agriculture, Forestry and Food of the Republic of Slovenia. Project number No. V4-0199-98. The funding is gratefully acknowledged.

References

BEVERLY, R. B., Y. C. HUNG, S. E. PRUSSIA, R. L. SCHWEFELT, E. W. TOLLNER, J. C. GARNER and D. ROBINSON (1987): Thermography as a non-destructive method to detect invisible quality damage in fruits and vegetables. Hort Science 22, 1056.

DALEY, P. F. (1995): Chlorophyll fluorescence analysis and imaging in plant stress and disease. Can. J. Plant Pathol. 17, 167–173.

GRAND D'ESNON A., G. RABATEL and R. PELLENC (1987): Magali: a self-propelled robot to pick apples. ASAE paper No. 87–1037.

HEMMING, J. and T. RATH (2002): Image processing for plant determination using the Hough transform and clustering methods. Gartenbauwissenschaften 67, 1–10.

INOUE, Y. (1990): Remote detection of physiological depression in crop plants with infrared thermal imagery. Japan Jour. Crop Sci. 59, 762–768.

INOUE, Y., B. A. KIMBALL, R. D. JACKSON, P. J. PINTER and R. J. REGINATO (1990): Remote estimation of leaf transpiration rate and stomatal resistance based on infrared thermometry. Agricultural and Forest Meteorology 51, 21–33.

JATUPHONG, V., M. H. GARY and L. B. ANDRE (2001): Thermal image bruise detection. ASAE Paper No. 01–6031.

KASSAY, L. (1992): Hungarian robotic apple harvester. ASAE Paper No. 92–7042.

KATAOKA, T., D. M. BULANON, T. HIROMA and Y. OTA (1999): Performance of Robotic Hand for Apple Harvesting. ASAE Paper No. 993003.

KONDO, N., K. HISAEDA and M. MONTA (1998): Development of Strawberry Harvesting. Robotic Hand, ASAE Paper No. 983117.

LAMBRECHTS, G. (2001): Apple EU 2001 Forecast 2001. Prognosfruit 2001, 1–8 http:cmlag.fgov.be/dg2/fr/Communications/prognos-algemeen.pdf.

LINKE, M., H. BEUCHE, M. GEYER and H. J. HELLEBRAND (2000): Possibilities and limits of the use of thermography for the examination of horticultural products. Agrartechnische Forschung 6, 110–114.

NILLSON, H. E. (1995): Remote sensing and image analysis in plant pathology. Can. J. Plant Pathol. 17, 154–166.

PARRISH, E. and A. K. GOKSEL (1977): Pictorial pattern recognition applied to fruit harvesting. Trans. ASAE 20, 822–827.

PEREZ, A. J., F. LOPEZ, J. V. BENLLOCH and S. CHRISTENSEN (2000): Colour and shape analysis techniques for weed detection in cereal feels. Comput. Electron. Agric. 25, 197–212.

RABATEL, G. (1988): A vision system for Magali, the fruit picking robot. Int. Conf. Agricultural Engineering, AGENG88, Paper 88293, Paris.

TOLLNER, E. W., J. K. BRECHT and B. L. UPCHURCH (1993): Non-destructive evaluation: Detection of external and internal attributes frequently associated with quality or damage. In "Post harvest-handling: a system approach". Food Science and Technology Series 7, 225–255.

WELTE, H. F. (1990): Forecasting harvest fruit size during the growing season. Acta Horticulturae 276, 275–282.

WINTER, F. (1979): Frupro1, a dynamical model connecting biological and economic elements of orchard management. Acta Horticulturae 97, 423–425.

WINTER, F. (1986): Modelling the biological and economic development of an apple orchard. Acta Horticulturae 160, 353–360.

ZHANG, S., T. TAKAHASHI and H. FUKUCHI (1997): Apple detection using infrared thermal imaging (part 1) – Thermal distribution on apple tree and acquisition of apple binary image. Journal of the Japanese Society of Agricultural Machinery (JSAM) 59, 57–64.

ZHANG, S., T. TAKAHASHI and H. FUKUCHI (1998a): Apple detection using infrared thermal imaging (part 2) – Detection method of apple using genetic algorithm. Journal of the Japanese Society of Agricultural Machinery (JSAM) 60, 69–76.

ZHANG, S., T. TAKAHASHI and H. FUKUCHI (1998b). Apple detection using infrared thermal imaging (part 3) – Real-time temperature measurement of apple tree. Journal of the Japanese Society of Agricultural Machinery (JSAM) 60, 89–95.

Addresses of authors

Assis. Lect. Denis Stajnko and **Assis. Prof. Miran Lakota**, University of Maribor, Faculty of Agriculture, Vrbanska 30, SI-2000 Maribor, Slovenia; e-mail: denis.stajnko@uni-mb.si

Dr. Marko Hočevar, University of Ljubljana, Faculty of Mechanical Engineering, Aškerčeva 6, SI-1000 Ljubljana, Slovenia

Assis. Prof. Zlatko Čmelik, University of Zagreb, Faculty of Agriculture, Svetošimunska cesta 25, HR-10000 Zagreb, Croatia

Eingelangt am 18. April 2003
Angenommen am 24. Jänner 2004